2005 International Linear Collider Workshop - Stanford, U.S.A.

Collider Signatures of Axino and Gravitino Dark Matter

Frank Daniel Steffen
DESY Theory Group, Notkestrasse 85, 22603 Hamburg, Germany

The axino and the gravitino are extremely weakly interacting candidates for the lightest supersymmetric particle (LSP). We demonstrate that either of them could provide the right amount of cold dark matter. Assuming that a charged slepton is the next-to-lightest supersymmetric particle (NLSP), we discuss how NLSP decays into the axino/gravitino LSP can provide evidence for axino/gravitino dark matter at future colliders. We show that these NLSP decays will allow us to estimate the value of the Peccei–Quinn scale and the axino mass if the axino is the LSP. In the case of the gravitino LSP, we illustrate that the gravitino mass can be determined. This is crucial for insights into the mechanism of supersymmetry breaking and can lead to a microscopic measurement of the Planck scale.

arXiv:hep-ph/0507003v1 30 Jun 2005

1. INTRODUCTION

A key problem in cosmology is the understanding of the nature of cold dark matter. In supersymmetric extensions of the Standard Model, the lightest supersymmetric particle (LSP) is stable if R-parity is conserved [1]. An electrically and color neutral LSP thus appears as a compelling solution to the dark matter problem. The lightest neutralino is such an LSP candidate from the minimal supersymmetric standard model (MSSM). Here we consider two well-motivated alternative LSP candidates beyond the MSSM: the axino and the gravitino.

In the following we introduce the axino and the gravitino. We review that axinos/gravitinos from thermal production in the early Universe can provide the right amount of cold dark matter depending on the value of the reheating temperature after inflation and the axino/gravitino mass. For scenarios in which a charged slepton is the next-to-lightest supersymmetric particle (NLSP), we discuss signatures of axinos and gravitinos at future colliders.

2. AXINOS AND GRAVITINOS

The axino $\widetilde{a}$ [2, 3, 4] appears (as the spin-1/2 superpartner of the axion) once the MSSM is extended with the Peccei–Quinn mechanism [5] in order to solve the strong CP problem. Depending on the model and the supersymmetry (SUSY) breaking scheme, the axino mass $m_{\widetilde{a}}$ can range between the eV and the GeV scale [3, 6, 7, 8]. The axino is a singlet with respect to the gauge groups of the Standard Model. It interacts extremely weakly as its interactions are suppressed by the Peccei–Quinn scale [9, 10] $f_a \gtrsim 5 \times 10^9\,\text{GeV}$. The detailed form of the axino interactions depends on the axion model under consideration. We focus on hadronic, or KSVZ, axion models [11] in a SUSY setting, in which the axino couples to the MSSM particles only indirectly through loops of additional heavy KSVZ (s)quarks.

The gravitino $\widetilde{G}$ appears (as the spin-3/2 superpartner of the graviton) once SUSY is promoted from a global to a local symmetry leading to supergravity (SUGRA) [12]. The gravitino mass $m_{\widetilde{G}}$ depends strongly on the SUSY-breaking scheme and can range from the eV scale to scales beyond the TeV region [1, 13, 14, 15]. In particular, in gauge-mediated SUSY breaking schemes [13], the mass of the gravitino is typically less than 100 MeV, while in gravity-mediated schemes [1] it is expected to be in the GeV to TeV range. Also, the gravitino is a singlet with respect to the gauge groups of the Standard Model. Its interactions—given by the SUGRA Lagrangian—are suppressed by the (reduced) Planck scale [10] $\text{M}_{\text{Pl}} = 2.4 \times 10^{18}\,\text{GeV}$. Once SUSY is broken, the extremely weak gravitino interactions are enhanced (for small values of the gravitino mass) through the super-Higgs mechanism.

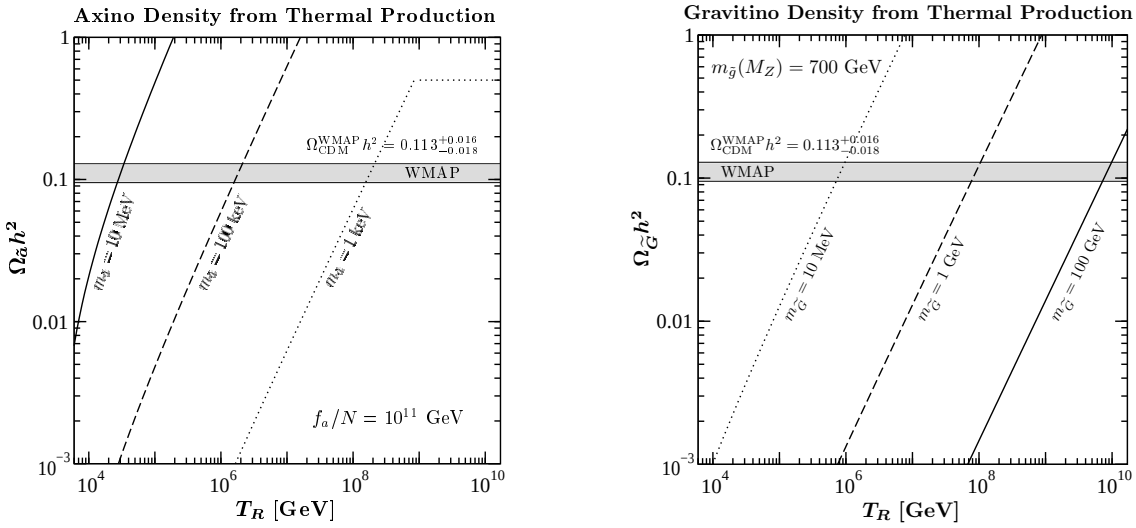

Figure 1: Relic densities of axino LSPs (left) and gravitino LSPs (right) from thermal production in the early Universe.

3. AXINOS AND GRAVITINOS AS COLD DARK MATTER

Because of their extremely weak interactions, the temperature T_D at which axinos/gravitinos decouple from the thermal plasma in the early Universe is very high. For example, an axino decoupling temperature of $T_D \approx 10^9$ GeV is obtained for $f_a = 10^{11}$ GeV. Gravitinos with $m_{\tilde G} \gtrsim 10$ MeV decouple at similar or even higher temperatures. Below the decoupling temperature, axinos/gravitinos can be produced in thermal reactions in the hot MSSM plasma. The thermal axino/gravitino production rate at high temperatures can be computed in a gauge-invariant way with the Braaten–Yuan prescription and hard thermal loop resummation, which takes into account Debye screening in the plasma. Assuming that inflation has diluted away any primordial axino/gravitino abundance, axino/gravitino-disappearance processes are negligible for a reheating temperature T_R sufficiently below T_D. The corresponding Boltzmann equation can be solved analytically. This leads to the following results for the relic densities $\Omega_{\tilde a/\tilde G} h^2$ of stable LSP axinos/gravitinos from thermal production [16, 17]

$$\Omega_{\tilde a} h^2 \;=\; 5.5\, g^6 \ln\left(\frac{1.108}{g}\right)\left(\frac{m_{\tilde a}}{0.1\ \text{GeV}}\right)\left(\frac{10^{11}\,\text{GeV}}{f_a/N}\right)^2\left(\frac{T_R}{10^4\,\text{GeV}}\right), \tag{1}$$

$$\Omega_{\tilde G} h^2 \;=\; 0.12\, g^2 \ln\left(\frac{1.163}{g}\right)\left(1+\frac{m_{\tilde g}^2}{3m_{\widetilde G}^2}\right)\left(\frac{m_{\widetilde G}}{100\ \text{GeV}}\right)\left(\frac{T_R}{10^{10}\,\text{GeV}}\right), \tag{2}$$

where h parametrizes the Hubble constant $H_0 = 100\, h$ km/s/Mpc, g is the strong coupling, N the number of heavy KSVZ (s)quark flavors, and $m_{\tilde g}$ the gluino mass. Note that $\Omega_{\tilde G} h^2$ increases with decreasing $m_{\widetilde G}$ due to enhanced gravitino interactions. The axino couplings do not depend on $m_{\tilde a}$ so that $\Omega_{\tilde a} h^2$ increases with increasing $m_{\tilde a}$.

In Fig. 1 we illustrate $\Omega_{\tilde a/\tilde G} h^2$ as a function of T_R for different values of $m_{\tilde a/\tilde G}$, where $f_a/N = 10^{11}$ GeV and $m_{\tilde g}(M_Z) = 700$ GeV. The running of the strong coupling and the gluino mass is taken into account by replacing g and $m_{\tilde g}$ in (1,2) respectively with $g(T_R) = [g^{-2}(M_Z) + 3\ln(T_R/M_Z)/(8\pi^2)]^{-1/2}$ and $m_{\tilde g}(T_R) = [g(T_R)/g(M_Z)]^2 m_{\tilde g}(M_Z)$, where M_Z is the Z-boson mass and $g^2(M_Z)/(4\pi) = 0.118$. For T_R above $T_D \approx 10^9$ GeV, $\Omega_{\tilde a} h^2$ is given by the equilibrium number density of a relativistic Majorana fermion and thus independent of T_R as shown for $m_{\tilde a} = 1$ keV. There will be a smooth transition instead of a kink once the axino-disappearance processes are taken into account. The grey band indicates the WMAP result [18] on the cold dark matter density (2σ error) $\Omega_{\rm CDM}^{\rm WMAP} h^2 = 0.113^{+0.016}_{-0.018}$. Axinos give the right amount of cold dark matter for $(m_{\tilde a}, T_R) = (100\,\text{keV}, 10^6\,\text{GeV})$. Higher values of T_R are problematic as $m_{\tilde a}$ becomes too light to explain structure formation. In contrast, gravitinos could provide the right amount of cold dark matter for combinations with a very high reheating temperature such as $(m_{\tilde G}, T_R) = (100\,\text{GeV}, 10^{10}\,\text{GeV})$. Nevertheless, other gravitino cold dark matter scenarios—such as $(m_{\tilde G}, T_R) = (10\,\text{MeV}, 10^6\,\text{GeV})$—are also viable.

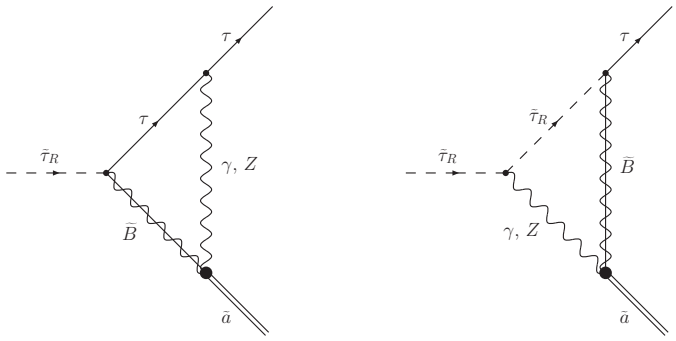

Figure 2: The 2-body decay $\widetilde{\tau}_{\rm R} \to \tau + \widetilde{a}$.

4. COLLIDER SIGNATURES OF AXINOS AND GRAVITINOS

As a consequence of the extremely weak couplings, the direct production of axino/gravitino LSPs at colliders is strongly suppressed. Furthermore, the NLSP typically has a long lifetime, which is subject to cosmological constraints as discussed, for example, in [19, 20]. At future colliders one expects a large sample of such quasi-stable NLSPs if the NLSP belongs to the MSSM spectrum. Each NLSP will eventually decay into the axino/gravitino LSP. These decays can provide signatures of axinos/gravitinos and other insights into physics beyond the MSSM (cf. [21, 22, 23, 24] and references therein). We concentrate on results extracted from Ref. [24] where more details can be found.

A significant fraction of the NLSP decays will take place outside the detector and will thus escape detection. For the charged slepton NLSP scenario, however, two recent works have proposed how such NLSPs could be stopped and collected for an analysis of their decays. It was found that up to $\mathcal{O}(10^3$–$10^4)$ and $\mathcal{O}(10^3$–$10^5)$ of charged NLSPs can be trapped per year at the Large Hadron Collider (LHC) and the International Linear Collider (ILC), respectively, by placing 1–10 kt of massive additional material around planned collider detectors [25, 26].

To be specific, we focus on the case where the pure 'right-handed' stau $\widetilde{\tau}_{\rm R}$ is the NLSP. We assume for simplicity that the neutralino-stau coupling is dominated by the bino coupling and that the lightest neutralino is a pure bino.

4.1. Probing the Peccei–Quinn Scale and the Axino Mass

In the axino LSP scenario, the total decay rate of the stau NLSP is dominated by the 2-body decay $\widetilde{\tau} \to \tau + \widetilde{a}$. In Fig. 2 we show the corresponding Feynman diagrams for the considered hadronic (KSVZ) axion models. The heavy KSVZ (s)quark loops are indicated as effective vertices by thick dots. The decay rate was estimated as [24]

$$\Gamma(\widetilde{\tau}_{\rm R} \to \tau\, \widetilde{a}) \simeq \xi^2\, (25\ {\rm s})^{-1} C_{\rm aYY}^2 \left(1 - \frac{m_{\tilde{a}}^2}{m_{\tilde{\tau}}^2}\right) \left(\frac{m_{\tilde{\tau}}}{100\,{\rm GeV}}\right) \left(\frac{10^{11}\,{\rm GeV}}{f_a}\right)^2 \left(\frac{m_{\tilde{B}}}{100\,{\rm GeV}}\right)^2 \ , \tag{3}$$

where $m_{\tilde{B}}$ is the mass of the bino and $m_{\tilde{\tau}}$ is the mass of the stau NLSP, i.e. $m_{\tilde{a}} < m_{\tilde{\tau}} < m_{\tilde{B}}$. The KSVZ-model dependence is expressed by $C_{\rm aYY} \simeq \mathcal{O}(1)$ and the uncertainty of the estimate is absorbed into $\xi \simeq \mathcal{O}(1)$. Thus, from the lifetime of the stau NLSP, $\tau_{\tilde{\tau}} \approx 1/\Gamma(\widetilde{\tau}_{\rm R} \to \tau\, \widetilde{a})$, an estimate of the Peccei–Quinn scale f_a can be obtained [24]

$$f_a^2 \simeq \left(\frac{\tau_{\tilde{\tau}}}{25\ {\rm s}}\right) \xi^2\, C_{\rm aYY}^2 \left(1 - \frac{m_{\tilde{a}}^2}{m_{\tilde{\tau}}^2}\right) \left(\frac{m_{\tilde{\tau}}}{100\,{\rm GeV}}\right) \left(\frac{m_{\tilde{B}}}{100\,{\rm GeV}}\right)^2 \left(10^{11}\,{\rm GeV}\right)^2 \ . \tag{4}$$

Indeed, we expect that $m_{\tilde{\tau}}$ and $m_{\tilde{B}}$ will already be known from other processes when the stau NLSP decays are analyzed. The dependence on $m_{\tilde{a}}$ is negligible for $m_{\tilde{a}}/m_{\tilde{\tau}} \lesssim 0.1$. For larger values of $m_{\tilde{a}}$, the stau NLSP decays can be used to determine the axino mass kinematically, i.e., from a measurement of the energy of the emitted tau E_τ,

$$m_{\tilde{a}} = \sqrt{m_{\tilde{\tau}}^2 + m_\tau^2 - 2 m_{\tilde{\tau}} E_\tau} \ , \tag{5}$$

where the error is given by the experimental uncertainty on $m_{\tilde{\tau}}$ and E_τ. The determination of both the Peccei–Quinn scale f_a and the axino mass $m_{\tilde{a}}$ is crucial for insights into the cosmological relevance of the axino LSP.

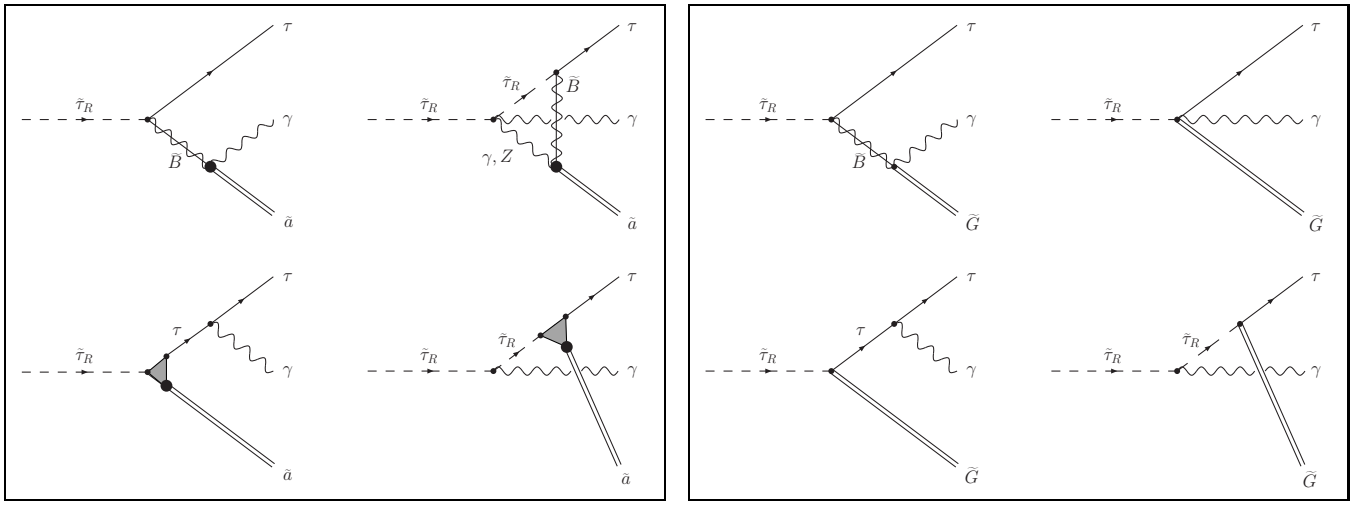

Figure 3: The 3-body decays $\widetilde{\tau}_{\rm R} \to \tau + \gamma + \widetilde{a}$ (left) and $\widetilde{\tau}_{\rm R} \to \tau + \gamma + \widetilde{G}$ (right).

4.2. Measuring the Gravitino Mass and the Planck Scale

In the gravitino LSP scenario, the main decay mode of the stau NLSP is the 2-body decay $\widetilde{\tau} \to \tau + \widetilde{G}$. Neglecting the τ mass, the following tree-level result for the decay rate is obtained from the SUGRA Lagrangian

$$\Gamma(\widetilde{\tau}_{\rm R} \to \tau\, \widetilde{G}) = \frac{m_{\tilde{\tau}}^5}{48\pi\, m_{\tilde{G}}^2\, {\rm M}_{\rm Pl}^2} \left(1 - \frac{m_{\tilde{G}}^2}{m_{\tilde{\tau}}^2}\right)^4 = (5.89\ {\rm s})^{-1} \left(\frac{m_{\tilde{\tau}}}{100\ {\rm GeV}}\right)^5 \left(\frac{10\ {\rm MeV}}{m_{\tilde{G}}}\right)^2 \left(1 - \frac{m_{\tilde{G}}^2}{m_{\tilde{\tau}}^2}\right)^4 \tag{6}$$

with the value of the reduced Planck mass ${\rm M}_{\rm Pl} = (8\pi\, G_{\rm N})^{-1/2} = 2.435 \times 10^{18}\,{\rm GeV}$ as given by macroscopic measurements of Newton's constant [10] $G_{\rm N} = 6.709 \times 10^{-39}\,{\rm GeV}^{-2}$. Thus, the gravitino mass $m_{\widetilde{G}}$ can be determined once the stau NLSP lifetime, $\tau_{\tilde{\tau}} \approx 1/\Gamma(\widetilde{\tau}_{\rm R} \to \tau\, \widetilde{G})$, and $m_{\tilde{\tau}}$ are measured. This will be crucial for insights into the SUSY breaking mechanism. If the gravitino mass can be determined independently from the kinematics via $m_{\tilde{G}} = (m_{\tilde{\tau}}^2 + m_\tau^2 - 2m_{\tilde{\tau}} E_\tau)^{1/2}$, the lifetime $\tau_{\tilde{\tau}}$ can also be used for a microscopic measurement of the Planck scale [23]

$${\rm M}_{\rm Pl}^2 = \frac{\tau_{\tilde{\tau}}}{48\pi} \frac{m_{\tilde{\tau}}^5}{m_{\tilde{G}}^2} \left(1 - \frac{m_{\tilde{G}}^2}{m_{\tilde{\tau}}^2}\right)^4 \ . \tag{7}$$

If consistent with macroscopic measurements, this would provide evidence for the existence of SUGRA in nature.

4.3. Distinguishing between Axinos and Gravitinos

A question arises as to whether one can distinguish between the axino LSP and the gravitino LSP scenarios. For $m_{\tilde{\tau}} = 100\,{\rm GeV}$ and $m_{\tilde{B}} = 110\,{\rm GeV}$, for example, the stau NLSP lifetime in the axino LSP scenario can range from $\mathcal{O}(0.01\ {\rm s})$ for $f_a = 5 \times 10^9\,{\rm GeV}$ to $\mathcal{O}(10\ {\rm h})$ for $f_a = 5 \times 10^{12}\,{\rm GeV}$. In the gravitino LSP case, the corresponding lifetime can vary over an even wider range, e.g., from $6 \times 10^{-8}\,{\rm s}$ for $m_{\widetilde{G}} = 1$ keV to 15 years for $m_{\widetilde{G}} = 50$ GeV. Thus, both a very short lifetime, $\tau_{\tilde{\tau}} \lesssim$ ms, and a very long one, $\tau_{\tilde{\tau}} \gtrsim$ days, will point to the gravitino LSP. On the other hand, if the LSP mass cannot be measured and the lifetime of the stau NLSP is within the range $\mathcal{O}(0.01\ {\rm s})$–$\mathcal{O}(10\ {\rm h})$, it will be very difficult to distinguish between the axino LSP and the gravitino LSP from the lifetime $\tau_{\tilde{\tau}}$ alone.

The situation is considerably improved when one considers the 3-body decays $\widetilde{\tau}_{\rm R} \to \tau + \gamma + \widetilde{a}/\widetilde{G}$. The Feynman diagrams of the dominant contributions are shown in Fig. 3, where thick dots represent heavy KSVZ (s)quark loops and shaded triangles the set of diagrams given in Fig. 2. From the corresponding differential rates [24], one obtains the differential distributions of the visible decay products. These are illustrated in Fig. 4 in terms of the quantity

$$\frac{1}{\Gamma(\widetilde{\tau}_{\rm R} \to \tau\,\gamma\, i\,; x_\gamma^{\rm cut}, x_\theta^{\rm cut})} \frac{d^2\Gamma(\widetilde{\tau}_{\rm R} \to \tau\,\gamma\, i)}{dx_\gamma d\cos\theta} \ , \quad i = \widetilde{a}, \widetilde{G} \ , \tag{8}$$

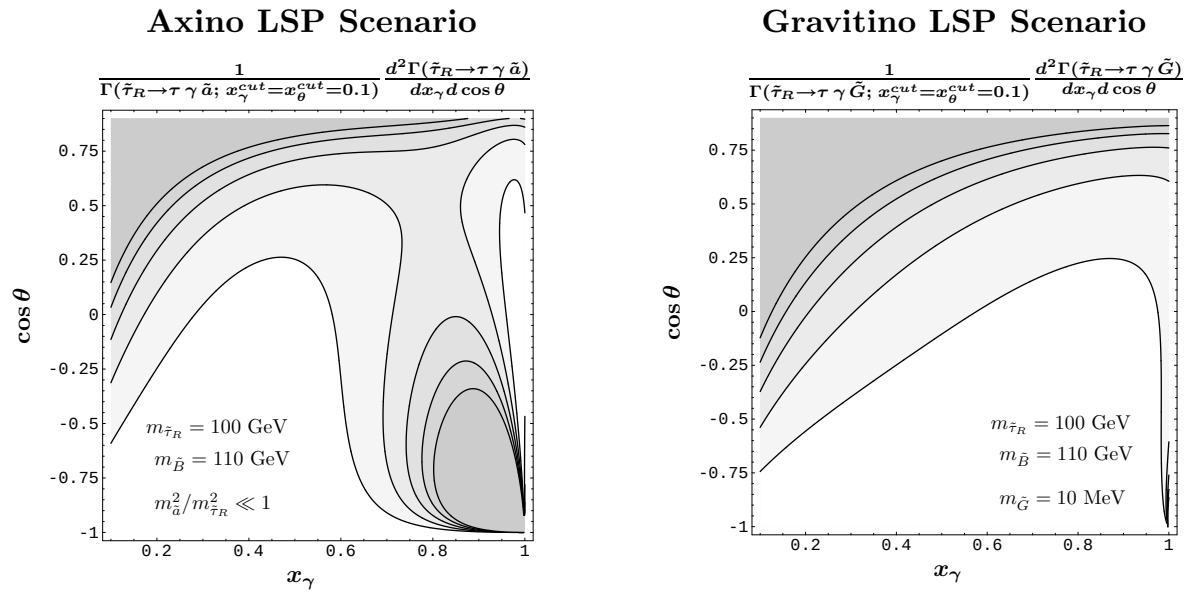

Figure 4: Differential distributions of the visible decay products in $\widetilde{\tau}_{\rm R} \to \tau + \gamma + \widetilde{a}$ (left) and $\widetilde{\tau}_{\rm R} \to \tau + \gamma + \widetilde{G}$ (right).

where $x_\gamma \equiv 2E_\gamma/m_{\tilde{\tau}}$ is the scaled photon energy, θ is the opening angle between the photon and tau directions, and

$$\Gamma(\widetilde{\tau}_{\rm R} \to \tau\,\gamma\,i\,; x_\gamma^{\rm cut}, x_\theta^{\rm cut}) \equiv \int_{x_\gamma^{\rm cut}}^{1-A_i} dx_\gamma \int_{-1}^{1-x_\theta^{\rm cut}} d\cos\theta\ \frac{d^2\Gamma(\widetilde{\tau}_{\rm R} \to \tau\,\gamma\,i)}{dx_\gamma d\cos\theta} \quad \text{with} \quad A_i \equiv \frac{m_i^2}{m_{\tilde{\tau}}^2} \tag{9}$$

is the respective integrated 3-body decay rate with the cuts $x_\gamma > x_\gamma^{\rm cut}$ and $\cos\theta < 1 - x_\theta^{\rm cut}$. Note that the quantity (8) is independent of the 2-body decay, the total NLSP decay rate, and the Peccei–Quinn/Planck scale.

The figure shows the normalized differential distributions (8) for the axino LSP with $m_{\tilde{a}}^2/m_{\widetilde{\tau}}^2 \ll 1$ (left) and the gravitino LSP with $m_{\widetilde{G}} = 10\,\text{MeV}$ (right), where $m_{\tilde{\tau}} = 100\,\text{GeV}$, $m_{\tilde{B}} = 110\,\text{GeV}$, and $x_\gamma^{\rm cut} = x_\theta^{\rm cut} = 0.1$. The contour lines represent the values 0.2, 0.4, 0.6, 0.8, and 1.0, where the darker shading implies a higher number of events. In the case of the gravitino LSP, the events are peaked only in the region where the photons are soft and the photon and the tau are emitted with a small opening angle ($\theta \simeq 0$). In contrast, in the axino LSP scenario, the events are also peaked in the region where the photon energy is large and the photon and the tau are emitted back-to-back ($\theta \simeq \pi$). Thus, if the observed number of events peaks in both regions, there is strong evidence for the axino LSP and against the gravitino LSP.

To be specific, with 10^4 analyzed stau NLSP decays, we expect about 165±13 (stat.) events for the axino LSP and about 100±10 (stat.) events for the gravitino LSP [24], which will be distributed over the corresponding $(x_\gamma, \cos\theta)$-planes shown in Fig. 4. In particular, in the region of $x_\gamma \gtrsim 0.8$ and $\cos\theta \lesssim -0.3$, we expect about 28% of the 165±13 (stat.) events in the axino LSP case and about 1% of the 100±10 (stat.) events in the gravitino LSP case. These numbers illustrate that $\mathcal{O}(10^4)$ of analyzed stau NLSP decays could be sufficient for the distinction based on the differential distributions. To establish the feasibility of this distinction, a dedicated study taking into account the details of the detectors and the additional massive material will be crucial, which we leave for future studies.

Some comments are in order. The differences between the two scenarios shown in Fig. 4 become smaller for larger values of $m_{\tilde{B}}/m_{\tilde{\tau}}$. This ratio, however, remains close to unity for the stau NLSP in unified models. Furthermore, if $m_{\tilde{G}} < m_{\tilde{a}} < m_{\tilde{\tau}}$ and $\Gamma(\widetilde{\tau} \to \widetilde{a}\,X) \gg \Gamma(\widetilde{\tau} \to \widetilde{G}\,X)$, one would still find the distribution shown in the left panel of Fig. 4. The axino would then eventually decay into the gravitino LSP and the axion. Conversely, the distribution shown in the right panel of Fig. 4 would be obtained if $m_{\tilde{a}} < m_{\tilde{G}} < m_{\tilde{\tau}}$ and $\Gamma(\widetilde{\tau} \to \widetilde{a}\,X) \ll \Gamma(\widetilde{\tau} \to \widetilde{G}\,X)$. Then it would be the gravitino that would eventually decay into the axino LSP and the axion. Barring these caveats, the signatures shown in Fig. 4 will provide a clear distinction between the axino LSP and the gravitino LSP scenarios.

5. CONCLUSIONS

Axino/gravitino LSPs from thermal production in the early Universe can provide the right amount of cold dark matter depending on their mass and the reheating temperature after inflation. If a charged slepton is the NLSP, future colliders can provide signatures of axino/gravitino LSPs and other insights into physics beyond the MSSM.

Acknowledgments

I am grateful to A. Brandenburg, L. Covi, K. Hamaguchi, and L. Roskowski for an enjoyable collaboration.

References

[1] H. P. Nilles, Phys. Rep. **110** (1984) 1;
H. E. Haber and G. L. Kane, Phys. Rep. **117** (1985) 75;
S. P. Martin, hep-ph/9709356.
[2] H. P. Nilles and S. Raby, Nucl. Phys. B **198** (1982) 102;
J. E. Kim and H. P. Nilles, Phys. Lett. B **138** (1984) 150.
[3] K. Tamvakis and D. Wyler, Phys. Lett. B **112** (1982) 451.
[4] J. E. Kim, Phys. Lett. B **136** (1984) 378.
[5] R. D. Peccei and H. R. Quinn, Phys. Rev. Lett. **38** (1977) 1440; Phys. Rev. D **16** (1977) 1791.
[6] J. F. Nieves, Phys. Rev. D **33** (1986) 1762.
[7] K. Rajagopal, M. S. Turner and F. Wilczek, Nucl. Phys. B **358** (1991) 447.
[8] T. Goto and M. Yamaguchi, Phys. Lett. B **276** (1992) 103;
E. J. Chun, J. E. Kim and H. P. Nilles, Phys. Lett. B **287** (1992) 123;
E. J. Chun and A. Lukas, Phys. Lett. B **357** (1995) 43.
[9] P. Sikivie, Nucl. Phys. Proc. Suppl. **87** (2000) 41.
[10] S. Eidelman *et al.* [Particle Data Group], Phys. Lett. B **592** (2004) 1.
[11] J. E. Kim, Phys. Rev. Lett. **43** (1979) 103;
M. A. Shifman, A. I. Vainshtein and V. I. Zakharov, Nucl. Phys. B **166** (1980) 493.
[12] J. Wess and J. Bagger, *Supersymmetry and supergravity* (Princeton University Press, Princeton, 1992).
[13] M. Dine, A. E. Nelson and Y. Shirman, Phys. Rev. D **51** (1995) 1362;
M. Dine, A. E. Nelson, Y. Nir and Y. Shirman, Phys. Rev. D **53** (1996) 2658;
G. F. Giudice and R. Rattazzi, Phys. Rep. **322** (1999) 419.
[14] L. Randall and R. Sundrum, Nucl. Phys. B **557** (1999) 79;
G. F. Giudice, M. A. Luty, H. Murayama and R. Rattazzi, JHEP **9812** (1998) 027.
[15] W. Buchmüller, K. Hamaguchi and J. Kersten, hep-ph/0506105.
[16] M. Bolz, A. Brandenburg and W. Buchmüller, Nucl. Phys. B **606** (2001) 518.
[17] A. Brandenburg and F. D. Steffen, JCAP **0408** (2004) 008; hep-ph/0406021; hep-ph/0407324.
[18] D. N. Spergel *et al.*, Astrophys. J. Suppl. **148** (2003) 175.
[19] L. Covi, L. Roszkowski, R. Ruiz de Austri and M. Small, JHEP **0406** (2004) 003.
[20] J. L. Feng, S. Su and F. Takayama, Phys. Rev. D **70** (2004) 075019.
[21] D. R. Stump, M. Wiest and C. P. Yuan, Phys. Rev. D **54** (1996) 1936.
[22] S. Ambrosanio, B. Mele, S. Petrarca, G. Polesello and A. Rimoldi, JHEP **0101** (2001) 014.
[23] W. Buchmüller, K. Hamaguchi, M. Ratz and T. Yanagida, Phys. Lett. B **588** (2004) 90; hep-ph/0403203.
[24] A. Brandenburg, L. Covi, K. Hamaguchi, L. Roszkowski and F. D. Steffen, Phys. Lett. B **617** (2005) 99.
[25] K. Hamaguchi, Y. Kuno, T. Nakaya and M. M. Nojiri, Phys. Rev. D **70** (2004) 115007.
[26] J. L. Feng and B. T. Smith, Phys. Rev. D **71** (2005) 015004.